International Journal of Innovation in Science and Mathematics
Volume 9, Issue 4, ISSN (Online): 2347–9051

# Research Based on the Influence Law of Flow Field Characteristics on Tire Hydroplaning Performance

**Hui Meng, Shicheng Lu, Aiqiang Li, Jing Wang, Yanhong Gao, Fei Pan and Congzhen Liu***
School of Transportation and Vehicle Engineering, Shandong University of Technology, Shandong, Zibo, Zhangdian, 255049, China.
*Corresponding author email id: lcz200811@163.com

*Date of publication (dd/mm/yyyy): 05/08/2021*

*Abstract* – **In order to improve the hydroplaning performance of automobile tires in rainy days, the tire hydroplaning mechanism was analyzed from the flow field characteristics in this paper. Based on the ANSYS workbench platform, a 185/60R15 vertical pattern tire-pavement shell model was established and the numerical results was analyzed by two-way flow-solid coupling algorithm. The relationship between flow velocity and the pressure field were obtained by observing the change of latter. Directions of water movements in the grooves and around the contact areas were learned by the method of water flow velocity vector decomposition. Besides, the mechanism of water flow vortex and the reasons of poor water fluidity at transverse and longitudinal grooves junction were explained. This paper proposes to strengthen the smoothness of the water flow in the grooves, weaken the influence of the water flow vortex, can improve the hydroplaning performance of the tire, and point out the direction for the optimization design of the tire groove.**

*Keywords* – **Tire Hydroplaning, Fluid-Solid Coupling, Dynamic Pressure, Flow Field Characteristics.**

## I. Introduction

The interaction between the tires and the pavement is the necessary basis for the dynamic characteristics of the automobile. As the only contact part of the driving pavement, its structural characteristics and use performance directly affect the performance of the whole vehicle. In rainy weather, when vehicles drive at high speed, the water flow cannot be discharged from the tire pattern groove in time, and the front of contact areas will produce dynamics pressure. When the speed is fast enough, the component of the vertical pressure is enough to balance the vertical load of the wheel, and the tire will be completely raised, and the phenomenon of tire hydroplaning occurs. Therefore, how to effectively improve the hydroplaning performance of vehicle tires and avoid traffic accidents as far as possible is an important problem for researchers to solve.

Researchers at home and abroad has made a preliminary exploration on the performance of hydroplaning from the theoretical aspect. Simulated several patterned tires and compared tire contact forces by Cho et al. showed that the tread patterns structure parameter determines anti-hydroplaning performance. Fwa et al. studied the effects of vertical and horizontal circumferential groove dimension on hydroplaning, indicating that unit tread pattern area can be used as evaluation of the performance of hydroplaning. Konghui Guo et al. applied the brush model to the research on the longitudinal skid of the tires on the water roads, comparing the water skid simulation results of the wet and dry road surface, the relationship between the tire longitudinal skid characteristics and the two different roads was clarified. Fluent software was used by Haichao Zhou et al. to make a simulation analysis of the tire hydroplaning fluid domain model, the tire hydroplaning mechanism and interference factors were elaborated, with the help of the bionic principle, the V-riblet bionic groove was applied to the bottom of the groove, so as to improve hydroplaning performance of tires.

Based on the ANSYS workbench platform, a 185/60R15 vertical pattern tire-pavement shell model was established and its effectiveness was verified through the radial stiffness test. Two-way flow-solid coupling algorithm was used to analyze the numerical results. In order to clarify the factors hindering the drainage of pattern, intervene in the simulation post processing analysis process from the perspective of flow field characteristics, clarify the obvious influencing factors of tires hydroplaning phenomenon, strengthen the smoothness of the water flow in contact areas, weaken the interference of water vortex, and effectively improve hydroplaning characteristics of tires.

## II. Establishment of Physical Model

The simulation method of tire hydroplaning based on ANSYS Workbench platform was adopted in this paper. With 185/60R15 tire, a finite element model was established in the solid module and the effective reliability of the fluid domain model was verified, the fluid domain model was built in the fluid module. Besides, the tire force deformation was applied to the fluid, and the dynamic pressure generated by the corresponding fluid acted to the tire in the system coupling module, to achieve the two-way flow-solid coupling.

### A. *Tire-Pavement Shell Model*

As the only part directly contacting with the road, tires have extremely complex internal components. Considering the actual requirements of this study, assumptions and modeling process for 185 / 60R15 was made as follows:

Table 2.1. Material parameters of tread and sidewall.

| **Component** | **Elastic Modulus/MPa** | | | **Shear Modulus /MPa** | | | **Density/(kg/m³)** | **Poisson Ratio** |
|---|---|---|---|---|---|---|---|---|
| | $E_a$ | $E_b$ | $E_c$ | $G_a$ | $G_b$ | $G_c$ | | |
| Tread/ Sidewall | 900 | 700 | 700 | 30 | 30 | 30 | 1200 | 0.45 |

Guided by the influence law of tire hydroplaning performance caused by tire pattern groove layout direction and pattern type, the tire-pavement finite element model was established, retaining the structure of tire pattern, sidewall and rim. Shell unit simulation analysis was selected for the tire-pavement shell model. The tire model is uniformly orthogonal anisotropic material; rim and pavement are rigid material, and the material parameters are shown in Table 2.1 and Table 2.2.

Table 2.2. Material parameters of rim and pavement.

| **Component** | **Density/(kg/m³)** | **Elastic Modulus/GPa** | **Poisson Ratio** |
|---|---|---|---|
| Rim | 2700 | 100 | 0.3 |
| Road | 2200 | 30 | 0.15 |

The single distance tire pattern was established through the relevant modeling software, imported into the transient structural mechanics module of the ANSYS Workbench platform; the contour line of the single distance tire pattern, tire side and rim rotate 360 along the rotation axis Y axis, forming a 3-dimensional housing model and combine the model into a component; the pavement housing model was established 1 mm from the center of the tread. Tire-pavement finite element model, as shown in Figure 2.1.

### B. *Verification of the Tire Finite Element Model*

It is necessary to verify the effectiveness of the tire model through the evaluation of the radial stiffness. The tire radial stiffness test platform and computer terminal equipment are shown in Figure 2.2. The test platform is based on the CSS-88100 tire loading test machine of Changchun test machine.

Fig. 2.1. Tyre-pavement 3d shell model.

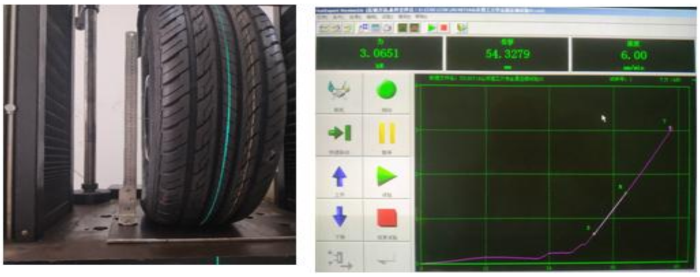

Fig. 2.2. Tire radial stiffness test.

The radial stiffness changes in stationary tires were simulated by loading on the ANSYS Workbench platform, as shown in Figure 2.3. The results of simulation are compared with radial deformation test and the radial stiffness change curve was completed, as shown in Figure 2.4. Judging from the figure, the radial stiffness simulation variation curve of the tire finite element model basically agrees with the corresponding experimental test scatter data, with a highly similar trend and a maximum relative error of 6.07%. This result strongly illustrated the effective reliability of the tire-pavement finite element model.

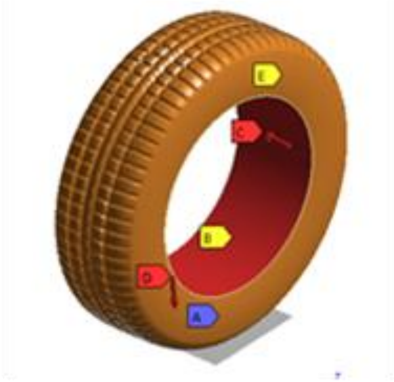

Fig. 2.3. Schematic diagram of radial stiffness loading condition of tire.

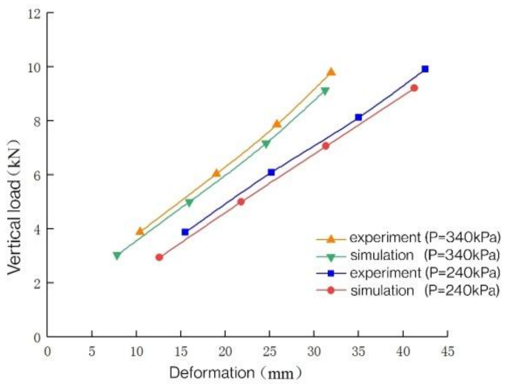


Fig. 2.4. Radial stiffness variation curve.

C. *Fluid Domain Model and Boundary Condition Setting*

A hexahedral model was established for the water layer and a boolean reduction operation was performed with the tire, and the rest is the fluid domain model. Then, grid mesh and boundary conditions were defined. The tetrahedral mesh division of the patch coordination method for the fluid domain in Fluent produces a total of 196,350 tetrahedral units and 40,333 nodes, as shown in Figure 2.5 (a). The boundary conditions of the fluid domain model are defined, and the motion of the profile file defined water was applied to the velocity inlet, as shown in Figure 2.5 (b).

(a) Fluid grid

(b) Boundary conditions.

Fig. 2.5. Fluid domain model and boundary conditions.

International Journal of Innovation in Science and Mathematics
Volume 9, Issue 4, ISSN (Online): 2347–9051

## III. Study on the Characteristics of the Tire Hydroplaning Fluid Flow Field

The tire hydroplaning simulation model established in section 2 was used this section, and two-way flow-solid coupling algorithm was applied to study the characteristics of the tire hydroplaning fluid flow field. Firstly, statatic characteristics and dynamic pressure characteristics of Vertical pattern tire at different times was analyzed, the conclusion that the pressure at the contact areas can increase as the flow speed increasing was obtained. So that the fluid flow constantly squeeze into the contact areas and then hydroplaning occurs. Last, the flow velocity characteristics, flow line and vortex distribution at different times was conducted and reasons of the vortex at the transverse trench outlet and the poor smoothness at the intersection of the transverse longitudinal groove are obtained.

### A. *Analysis of the Flow Field Pressure Characteristics*

The cloud map of different depths and moments was selected in this paper to explore the influence of water layer depth and flow velocity on the pressure around the tire.

#### a. *The Influence of Water Layer Depth on the Pressure around the Tire*

(1) Z direction analysis and selection of the static pressure cloud map.

Figure 3.1 shows a static pressure cloud map of the fluid domain at different depths under constant motion of 30 m/s water flow. As can be seen in the figure, under different water layer depth value of Z direction, when the depth value of the water layer increases, the static pressure value and distribution also increase accordingly.

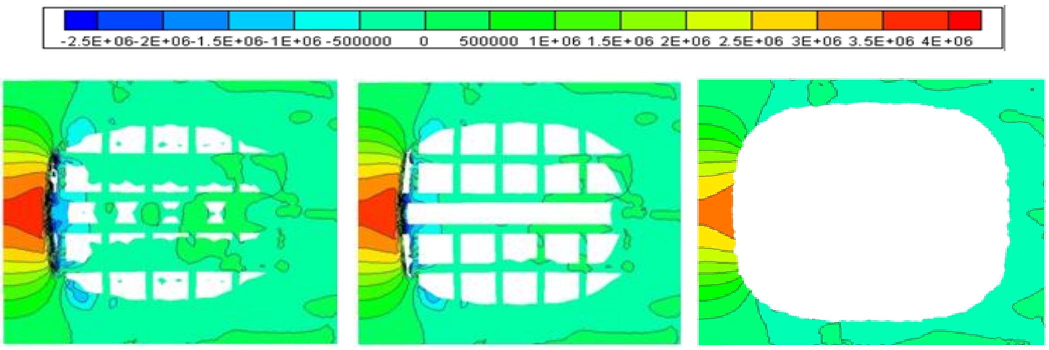


2mm 4mm 8mm

Fig. 3.1. Hydrostatic pressure nephogram of fluid domain at different depths domain.

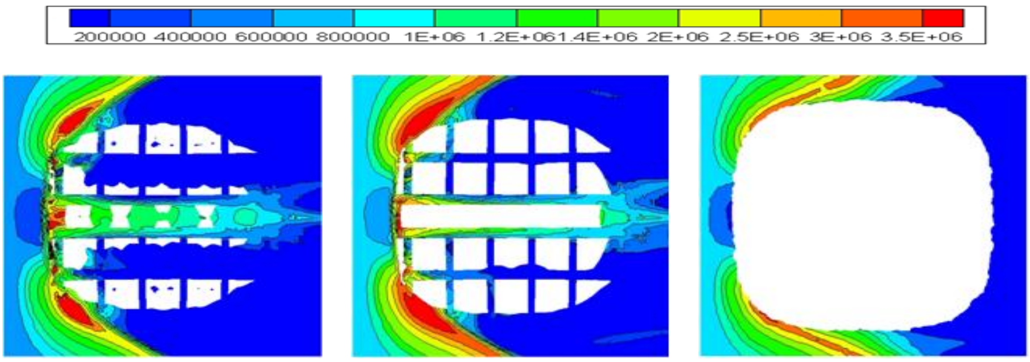


2mm 4mm 8mm

Fig. 3.2. Hydrodynamic pressure nephogram of fluid domain.

(2) Z direction analysis and selection of the dynamic pressure cloud map.

As the dynamic pressure cloud map in different locations shown in Figure 3.2, dynamic pressure increases in the value and distribution area with the depth. The closer the flow to the upper and lower walls of the fluid domain, the closer the particle velocity is to zero. Because the moving water pressure of the fluid is proportional to the square of the flow velocity, the particle velocity of the central region of the water layer is large, so that the dynamic pressure is formed.

From the cloud map at the 4 mm plane, in terms of the distribution of dynamic water pressure, it is still mainly concentrated at the grounding front edge of the tread shoulder and at the center of the grounding front edge, clearly showing the value change and distribution of moving water pressure in the groove in the pattern coupling area. Therefore, it is appropriate to intercept the dynamic water pressure cloud map away from the road surface 4 mm plane in the Z direction.

b. *The Influence of Water Flow Velocity on the Pressure around the Tire*

(1) Analysis of flow velocity on dynamic pressure

According to the corresponding dynamic pressure cloud Figure 3.3 at different times, that within a certain range, the water flow continuously hits the front edge of the grounding area, thus gradually increasing the concentrated water pressure at the shoulder of the front edge of the tire.

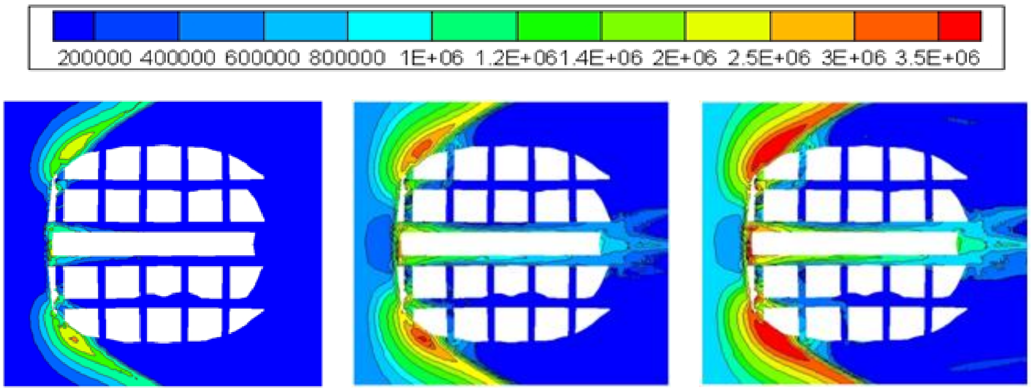


t = 0.8 s t = 1.0 s t = 1.2 s

Fig. 3.3. Hydrodynamic pressure nephogram at different time.

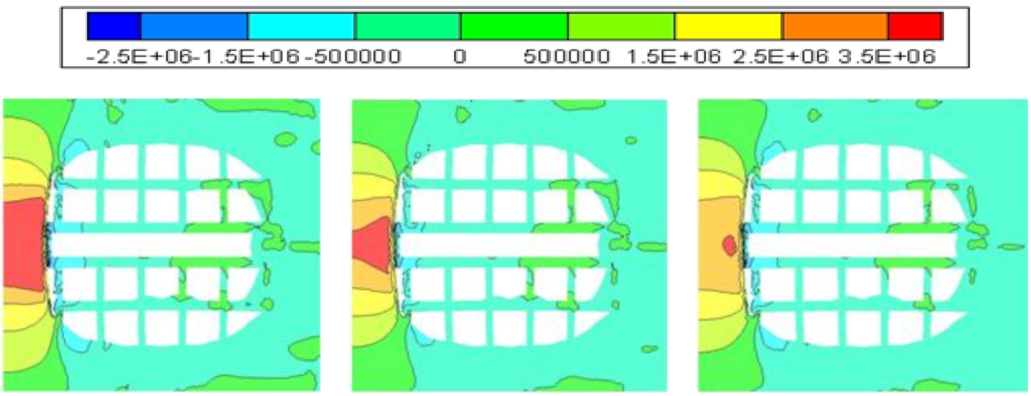


t = 0.8 s t = 1.0 s t = 1.2 s

Fig. 3.4. Hydrostatic pressure nephogram at different time.

(2) Analysis of flow velocity on static pressure.

It is seen from Fig. 3.4 that when the water flow velocity rises within a certain range, the tire tread pattern corresponding to the three moments decreases in turn with the front edge of the road surface contact area and the two static pressure concentration areas formed at the rear of the road surface contact area.

## B. *Analysis of Water Flow Characteristics*

In order to further explore the hydroplaning mechanism of the tire and draw the reason for the formation of a huge vortex at the transverse groove outlet, the velocity characteristics, the streamline and the vortex flow characteristics of the vertical tread tire were tried to explain the hydroplaning problem.

### a. *Analysis of Velocity Characteristics*

To observe the change of water flow in the whole contact area and surrounding flow field and study the velocity in the vertical pattern groove, the velocity distribution cloud map and the water flow motion vector map at 30 m/s at 4 mm from the conclusion of the previous section. Considering that both sides of the fluid domain and the exits are pressure exits, it is necessary to show the flow velocity vector of the X-Y plane, i.e., the longitudinal velocity component VY and the transverse velocity component VX, are shown in Figure 3.5 and 3.6.

Figure 3.5 shows the $V_Y$ contour diagram, revealing that the longitudinal velocity $V_Y$ of the water flow at the edge of the longitudinal pattern groove, and the entrance of the longitudinal pattern groove extends along the longitudinal pattern groove to the rear of the pattern connection area. Thus, from the perspective around the pattern contact area, the edge of the shoulder is a main drainage area; from the perspective of the contact area, the longitudinal pattern groove, especially the central of it, is another main drainage area.

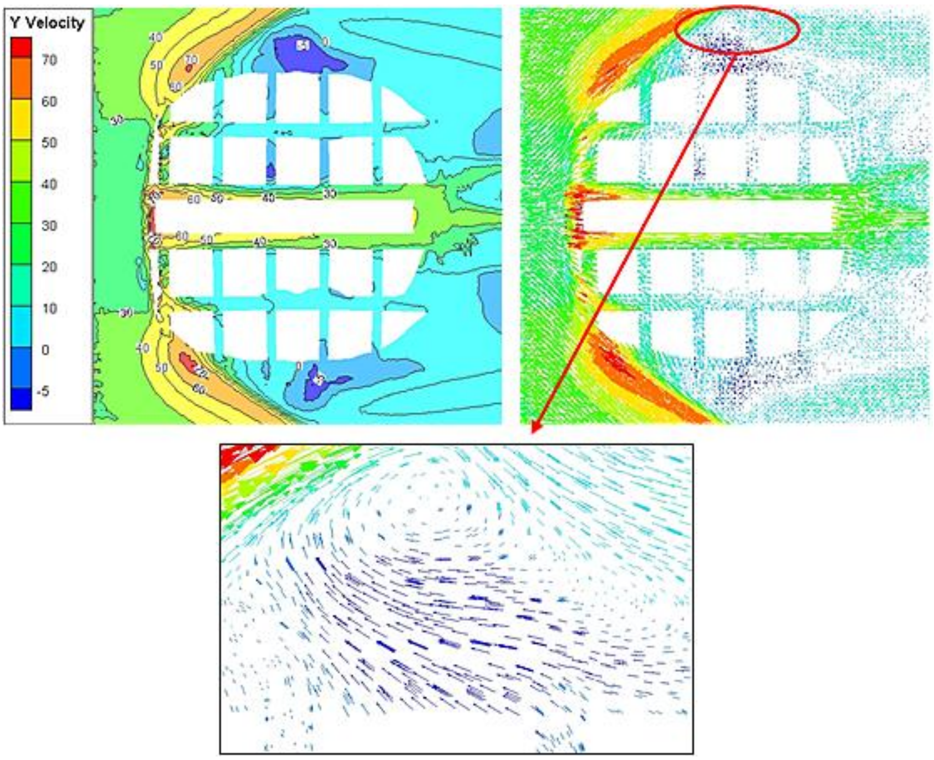


Fig. 3.5. The longitudinal distribution of water velocity.

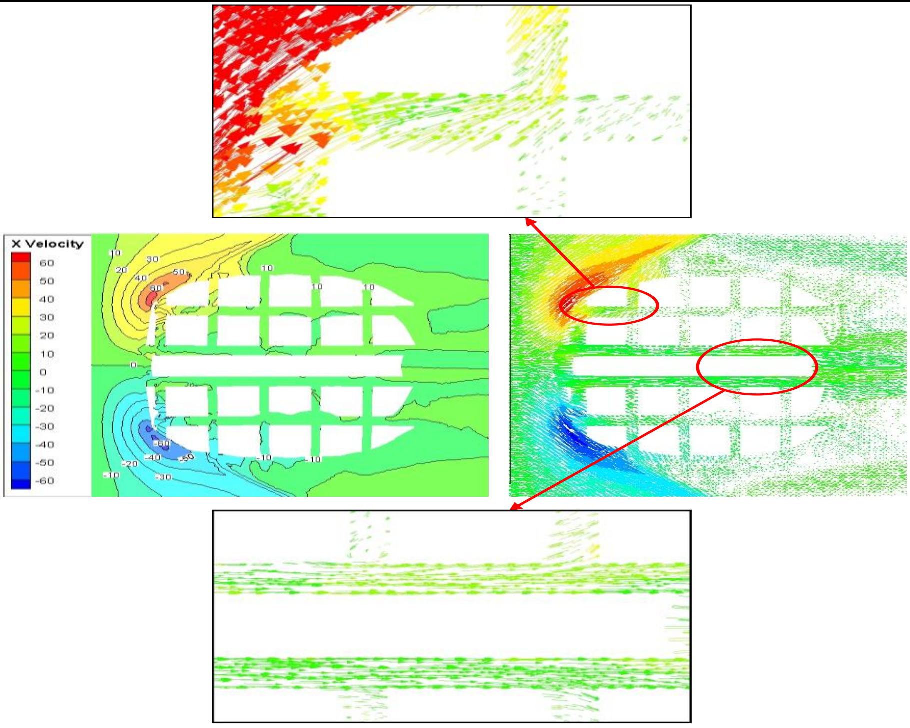


Fig. 3.6. The transverse distribution of water velocity.

According to Figure 3.6, the grounding area and surrounding transverse velocity components are numerical below the longitudinal velocity component, which shows that the trend of large water flow is discharged along the Y direction from the rear exit in the contact area; in the central longitudinal pattern groove, the transverse velocity component shows that the flow velocity direction basically matches the groove direction and the flow is relatively smooth; the transverse velocity component of the rear grounding area is significantly increased, which has adverse effect on the timely elimination of water flow.

b. *Analysis of Flow Line and Vortex Characteristics*

The distribution of water flow lines at a constant speed of 30 m/s at 4 mm from the pavement is showed in Figure 3.7. It can be observed that the water movement of the vertical pattern tread at the front end of the grounding area, especially in the central longitudinal pattern groove and the inside, causing the water flow of the back part and the ground area, which is not conducive to the water sliding characteristics of the tire.

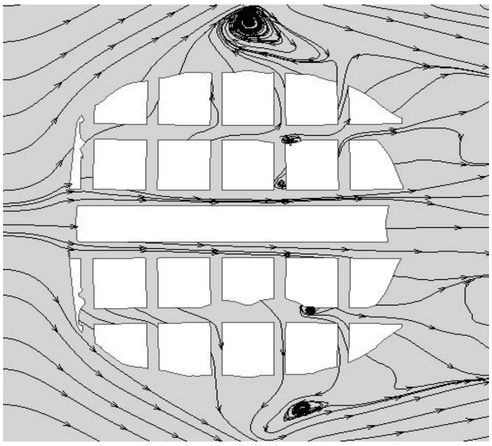

Fig. 3.7. Distribution of streamline.

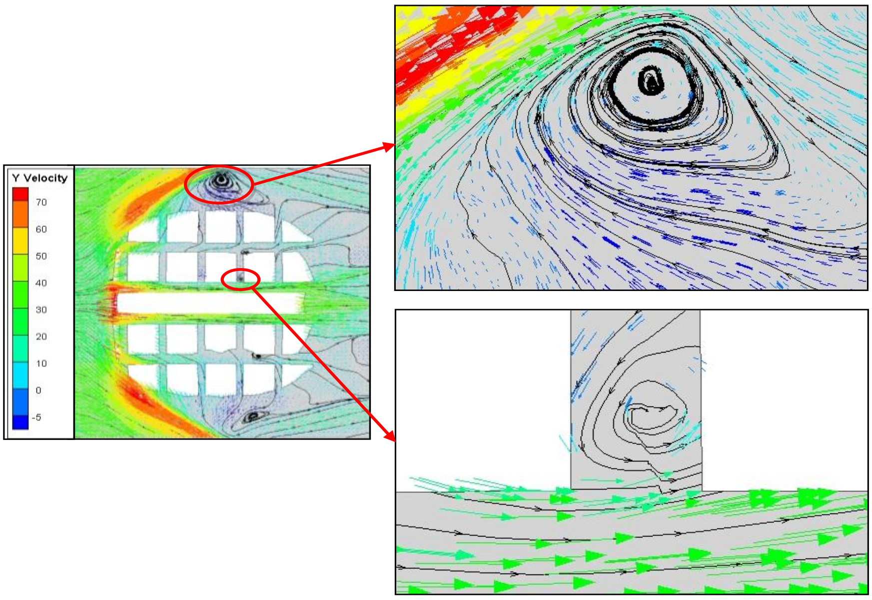


Fig. 3.8. Distribution of flow vortices.

Considering the complex movement of water flow in the grounding area, a single flow streamline diagram is insufficient and combined with the longitudinal velocity vector diagram of the flow. As shown in Figure 3.8, the water flow speech at the front edge of the grounding tire shoulder is high, known by the Bernoulli equation, the nearby static pressure drops, the transverse pattern groove water is discharged from the outlet, part of the water flow will reverse to the low pressure area, creating a huge vortex here.

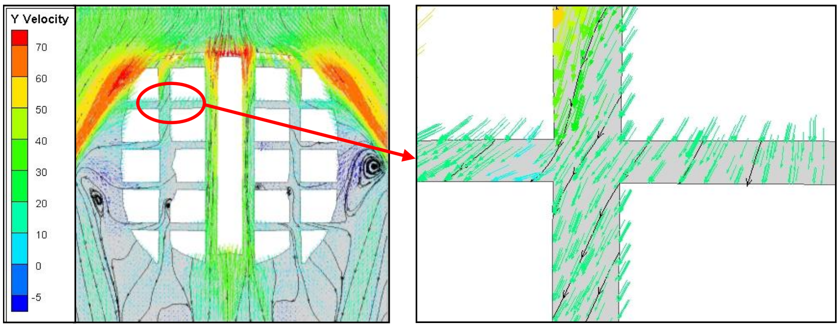


Fig. 3.9. Distribution of water flow in pattern grooves.

The motion state of the velocity vector in the tire grounding area is analyzed. As shown in Fig. 3.9, the water mass movement of the tire in the grounding longitudinal groove is more smooth than the transverse longitudinal groove, especially the central longitudinal pattern groove is more obvious. The transverse pattern trench found that the movement direction of the water mass point in the transverse ditch and the direction of the transverse ditch were too large, leading to the continuous impact on the wall of the trench, which not only weakened the drainage of the trench, but also caused the rise of dynamic water pressure in the area. Therefore, the angle between the transverse trench and the longitudinal groove is one of the reasons affecting the water skiing performance of the tire.

## IV. Conclusion

Based on two-way flow-solid coupling method, the post processing analysis process was completed in this paper to further explore the mechanism of tire hydroplaning on water roads, intervenes in the exploration process from the perspective of flow field characteristics, the obvious interference factors of tire hydroplaning phenomenon were clarified and the following conclusions were obtained.

(1) By comparing the static pressure cloud map of different water layer depths, it was found that the flow field pressure around the contact areas and the main pattern groove can be fully observed at Z in 4mm. Taking it as the cloud map analysis plane, the corresponding pressure cloud map at different moments were obtained and the relationship between flow velocity and pressure field was learned;

(2) In terms of the fluid flow characteristics, the X-Y plane was used to decompose the water flow velocity vector, learning that the tire shoulder edge and the longitudinal pattern groove, especially the central longitudinal pattern groove, is the main drainage area;

The method of combining flow diagram and velocity vector diagram was used in this paper, and the cause of flow vortex at the outlet of transverse groove and poor water flow at the intersection of vertical and transverse pattern groove were clarified. It is proposed to strengthen the smoothness, weaken the influence of water vortex, improve the hydroplaning performance of the tire and point out the direction for the optimization design of tire groove.

## References

[1] Grogger H., Weiss M. Calculation of the three-dimensional free surface flow around an automobile tire [J]. Tire Science and Technology, 1996, 24(1): 39-49.
[2] Seta E., Nakajimay, Kamegawa T., et al. Hydroplaning analysis by FEM and FVM: Effect of tire rolling and tire pattern on hydroplaning [J]. Tire Science and Technology, 2000, 28(3): 140-156.
[3] Nakajima Y, Seta E. Hydroplaning analysis by FEM and FVM, effect of tire rolling and tire pattern on hydroplaning [J]. International Journal of Automatic Techno logy, 2000, 1(1): 26-34.
[4] Okano T., Koishi M.A. new computational procedure to predict transient hydroplaning performance of a tire [J]. Tire Science and Technology, 2001, 29(1): 2-22.
[5] Cho J.R., Lee H.W., Sohn J S, et al. Numerical investigation of hydroplaning characteristics of three-dimensional patterned Tire [J]. European Journal of Mechanics A/Solids, 2006, 25(2006): 914-926.
[6] Ong G.P., Asce A.M., Fwa T.F., et al. Wet-pavement hydroplaning risk and skid resistance modeling [J]. Journal of Transportation Engineering, 2007, 133(10): 590-598.
[7] Vincent S., Sarthou A., Caltagirone J.P., et al. Augmented lagrangian and penalty methods for the simulation of two-phase flows interacting with moving solids. Application to hydroplaning flows interacting with real tire tread patterns [J]. Journal of Computational Physics, 2011, 230(4): 956-983.
[8] Alhendal Y., Turan A., Aly W.I.A. VOF simulation of marangoni flow of gas bubbles in 2D-axisymmetric column[J]. Procedia Computer Science, 2010, 1(1): 673-680.
[9] Kumar S.S., Anupam K., Scarpas T, et al. Study of hydroplaning risk on rolling and sliding passenger car [J]. Procedia-Social and Behavioral Sciences, 2012, 53: 1019-1027.
[10] Jonas S., Artras K., Rolandas M., et al. Research of the influence of tire hydroplaning on directional stability of vehicle [J]. Proceedings of the Institution of Civil Engineers: Transport, 2013, 28(4): 374-380.
[11] Haichao Zhou et al. Numerical investigation of passive control flow to improve tire hydroplaning performance using a V-riblet non-smooth surface [J]. Advances in Mechanical Engineering, 2017, 9(11)
[12] Zheng B.S., Huang X.M., Zhang W.G., et al. Adhesion characteristics of tire-asphalt pavement interface based on a proposed tire hydroplaning model [J]. Advanced in Materials Science and Engineering, 2018, 1687-8434.

## Author's Profile

**First Author**
**Hui Meng,** Master in reading, Male, School of Transportation and Vehicle Engineering, Shandong University of Technology, Shandong, Zibo, Zhangdian, 255049, China. email id: 193286172@qq.com

**Second Author**
**Shicheng Lu,** Master in reading, Male, School of Transportation and Vehicle Engineering, Shandong University of Technology, Shandong, Zibo, Zhangdian, 255049, China. email id: 2232416378@qq.com

**Third Author**
**Aiqiang Li,** Master in reading, Male, School of Transportation and Vehicle Engineering, Shandong University of Technology, Shandong, Zibo, Zhangdian, 255049, China. email id: laq199897@163.com

**Fourth Author**
**Jing Wang,** Bachelor, Female, Technology Center, Shandong Tangjun Ouling Automobile Manufacture Co., Ltd., Shandong, Zibo, Zichuan, 255000, China.

**Fifth Author**
**Yanhong Gao,** Bachelor, Female, Technology Center, Shandong Tangjun Ouling Automobile Manufacture Co., Ltd., Shandong, Zibo, Zichuan, 255000, China.

**Sixth Author**
**Fei Pan,** Master, Female, Department of Vehicle Operation Engineering, Yantai Automobile Engineering Professional College, Shandong, Yantai, Fushan, 265500, China.

**Seventh Author**
**Congzhen Liu,** Doctor of Engineering, Male, Associate professor (Correspondence author), School of Transportation and Vehicle Engineering, Shandong University of Technology, Shandong, Zibo, Zhangdian, 255049, China.